PHYSICAL REVIEW C **74**, 031301(R) (2006)

Nuclear excitation by electron transition on ^{197}Au by photoionization around the K-absorption edge

S. Kishimoto,[1] Y. Yoda,[2] Y. Kobayashi,[3] S. Kitao,[3] R. Haruki,[4] R. Masuda,[3] and M. Seto[3]
[1]*Institute of Materials Structure Science, KEK, Tsukuba, Ibaraki 305-0801, Japan*
[2]*Japan Synchrotron Radiation Research Institute, Sayo, Hyogo 679-5198, Japan*
[3]*Research Reactor Institute, Kyoto University, Kumatori, Sennan, Osaka 590-0494, Japan*
[4]*Research and Development Center for Higher education, Kyushu University, Ropponmatsu, Fukuoka 106-8558, Japan*
(Received 17 October 2005; revised manuscript received 27 May 2006; published 21 September 2006)

We have observed nuclear excitation by electron transition (NEET) on ^{197}Au by photoionization using synchrotron monochromatic x-rays around the K-absorption edge. By scanning the energy of the incident photons, we found that the NEET events had a steep edge at an energy (40 $\pm$ 2)eV higher than the K edge; its width (FWHM) was 14 $\pm$ 9 eV, quite narrower than that of the K edge. A fine structure of the NEET events was also observed at photon energies higher than the NEET edge. This behavior is explained by the atomic transition from a particular K-hole state to the M_1-hole state, which resonantly excites the nucleus, and by an outgoing photoelectron with energy conservation.

DOI: 10.1103/PhysRevC.74.031301 PACS number(s): 23.20.Nx, 25.20.Dc, 27.80.+w, 82.80.Ej

Nuclear excitation by electron transition (NEET) on ^{197}Au was certainly observed at an energy above the K absorption edge by using synchrotron radiation [1]. NEET on ^{197}Au occurs between the $K \rightarrow M_1$-hole atomic transition ($1S_{1/2}$: 80.725 keV $\rightarrow 3S_{1/2}$: 3.425 keV) and the $3/2^+ \rightarrow 1/2^+$ nuclear transition ($0 \rightarrow 77.351$ keV [2]). The transitions have energies close to each other, and for the same multipolarity of $M1$. A NEET model has explained this phenomenon by assuming an initial state consisting of an atomic inner-shell hole as well as a ground-level nucleus, and a final state consisting of an outer-shell hole and an excited nucleus, not considering the atomic excitation process [3–5]. Within the framework of the model, NEET on ^{197}Au can occur even at an energy below the K edge due to a finite K-shell width. However, in the year of 2001 after the experiment reported in Ref. [1], we observed that NEET events started to increase above the gold K-edge by varying the energy of the incident photons. Moreover, the NEET events had a leading edge steeper than the K edge and a fine structure existing at higher energies, although the results had poor statistics [6]. The existing NEET model cannot explain these facts because it does not include a process generating the inner-shell hole state by x-rays changing energy. Recently, we again observed the same behavior as that observed in 2001 with improved detector efficiency. We report on the results, and suggest an interpretation to explain them.

The experiment was carried out at undulator beamline BL09XU of SPring-8 during a period in April 2001 (Exp. I). After improving the detector efficiency, we conducted the same measurements as Exp. I, in October 2004 (Exp. II). During both periods, the SPring-8 ring was operated in a 203-bunch mode (bunch period: 23.6 ns). The experimental setup was almost the same as described in Ref. [7]. In Exp. II, the third-order x-rays from a diamond (111) double-crystal monochromator were used, instead of a Si(111) double-crystal monochromator. The x-ray beam was defined by slits of $^{V}1.0 \times {}^{H}1.0$ mm^2. A target of gold foil (3 μm thick) and a silicon avalanche diode (Si-AD, Hamamatsu SPL1401) were installed in a vacuum chamber in Exp. I, while a 1-μm gold foil and a couple of Si-AD arrays (Hamamatsu SPL2764) were used in Exp. II. Each gold foil was 99.9% in purity. The target was loaded from the top of the chamber with a linear-motion probe and inclined at 30° to the incident beam. The Si-AD of SPL1401 was 3 mm in diameter and had a depletion region 30 μm thick, while the Si-AD array had three pixels of 1×6 mm^2 (pitch: 1.1 mm), a depletion region 30 μm thick. The Si-AD in each experiment was located 2.5 mm apart from the center of the target, on the horizontal plane; the pixel of each Si-AD array was set in parallel with the incident beam, at the upstream or downstream side of the target. Radiation just emitted from excited nuclei, especially the L-internal conversion electron (maximum energy: 63 keV), was mainly detected by the Si-AD. We provided a thin SiO_2 layer of less than 25 nm at the front surface of each Si-AD, for detection of the conversion electrons without a large energy loss. A fast amplifier of gain 100 (Phillips Scientific 6954) was connected to each channel of the Si-AD and outputted a pulse of about 40 mV in maximum pulse-height and of 2-ns width, for the conversion electron. In Exp. II, three outputs from each pixel of the array were added together in a fan-in/fan-out module (LeCroy 429A), after processed in a constant-fraction discriminator (ORTEC 935). A time gate selected the pulse timing of the conversion electrons after piling-up of pulses by the atomic radiation. The time spectra and the time-gated counts were independently recorded in each array, that is ch-A at the upstream side or ch-B at the downstream side. A pair of silicon PIN photodiodes (Hamamatsu M6906), 5×5 mm^2 in size and 500 μm thick, of transmission type was used in both experiments to monitor the incident-beam intensity. One of the photodiodes (I_0) was located in front of the chamber and the other (I) was attached behind the target inside the chamber.

In these experiments, by scanning the energy of the monochromator, we first observed nuclear resonance at 77.3 keV, directly excited by the incident x-rays. Figure 1 shows peak profiles of the delayed counts with steps of 2 eV in

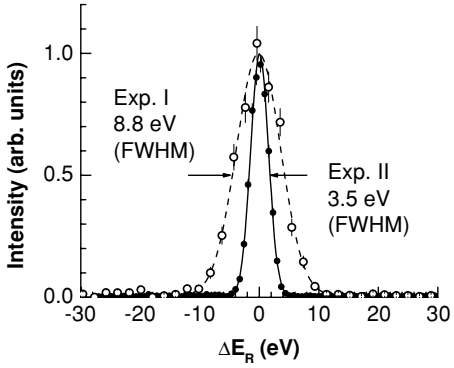

FIG. 1. Peak profiles of the delayed counts observed at nuclear resonance ($\Delta E_R = 0$) in Exp. I (open circles) and Exp. II (closed circles) by scanning the monochromator energy. The scanning step was 2 eV or 0.7 eV, respectively. The widths (FWHM) were obtained by a least-squares fitting of a Gaussian.

Exp. I, or 0.7 eV in Exp. II. The delayed counts were measured for 30 s per point, while gating for a time region of 3.7–18 ns after a timing for the atomic transition. The count rate in Exp. II reached 33 counts/s with the sum of the ch-A and B. The efficiency of the Si-AD arrays was about 4.3-times higher than that of a single Si-AD in Exp. I, considering the beam width, the beam intensity and the thickness of the targets. Each peak was fitted by a Gaussian, and the full width at half maximum (FWHM) was 8.8 ± 0.2 eV in Exp. I, or 3.5 ± 0.1 eV in Exp. II. The incident-photon energy (E) was calculated from the angle of the monochromator. The value of ΔE_R ($=E - E_R$) was decided by assuming that the resonance occurred at $E_R = 77.351$ keV. The intensity in Fig. 1 is given by normalizing the fitted counts at $\Delta E_R = 0$ eV. Note that the peak widths were broadened by the energy resolution of the beamline optics, while the natural width of the nuclear excited level was quite narrow, 2.39×10^{-7} eV, obtained from the 1.91-ns half-life of the 77.3-keV state [2].

Figure 2 shows the time spectrum of radiation from the decaying nuclei, measured at the resonance ($\Delta E_R = 0$ eV) in Exp. II using signals of the ch-A (closed circles). The

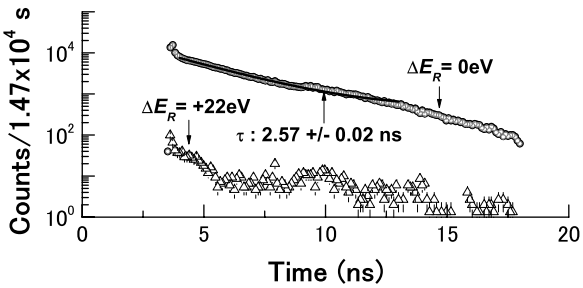

FIG. 2. Time spectrum observed in Exp. II using the ch-A for nuclear resonance at $\Delta E_R = 0$ eV during 14700 s (closed circles). The background (triangles) was measured at $\Delta E_R = +22$ eV. The net spectrum (open circles) was obtained by subtracting the background from the data recorded at $\Delta E_R = 0$ eV, after being normalized by the incident-photon number. The solid curve shows a decay with a time-constant $\tau(= 2.57 \pm 0.02$ ns) for the net data of 4.5–13 ns by a least-squares fitting.

measuring time was 14700 s. Another spectrum, indicated by triangles, was measured to estimate the background, at $\Delta E_R = +22$ eV, 6.3 times as large as the beam width, higher than the resonance energy. The net counts were obtained by subtracting the data obtained at $\Delta E_R = +22$ eV from those measured at $\Delta E_R = 0$ eV, while normalizing the delayed counts by the number of the incident photons calculated by the output I. The net counts, plotted by open circles, almost overlapped with the data observed at $\Delta E_R = 0$ eV. The solid curve in Fig. 2 was given by a fitting of the exponential decay of $y_0 + \exp(-t/\tau)$ for the data between 4.5 and 13 ns. By a least-squares fitting, a value of τ, 2.57 ± 0.02 ns, was obtained. Compared with the lifetime of $\tau_0 = 2.75$ ns for the 77.3-keV level, it was about 10% shorter. It may be affected by the time structure of a steep tail, which was caused by huge prompt pulses of atomic radiation. The term y_0 was also needed for the residual effect of the huge prompt pulses, even after subtracting the background.

We next observed the delayed-events of NEET as a function of the incident-photon energy around the K-absorption edge. The numbers of the delayed events, N_{de}, are given in Fig. 3: (a) for Exp. I and (b) for Exp. II. The time region for the delayed counts was the same as in the measurement for the resonance. The integral measuring time per point was 550 s in Exp. I and 500 s in Exp. II, as a sum of eleven and ten scans, respectively. The energy of the K-absorption edge (E_K) was assumed to be 80.725 keV [8]; ΔE_K was defined by $E - E_K$. In Exp. I, the scanning range and the step were $-220\,\text{eV} < \Delta E_K < +464$ eV and 12 eV, respectively, while $-209\,\text{eV} < \Delta E_K <$

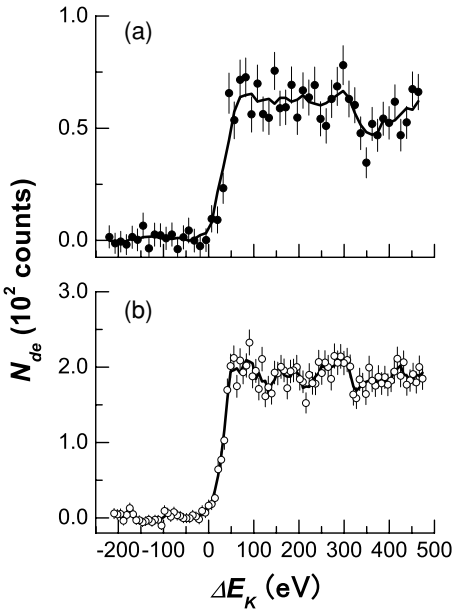

FIG. 3. Number of delayed events as a function of ΔE_K (where $\Delta E_K = 0$ eV means the gold K-edge): (a) for Exp. I and (b) for Exp. II. The scanning range and the step were -220 eV $< \Delta E_K <$ +464 eV and 12 eV in (a), -209 eV $< \Delta E_K <$ +474 eV and 7 eV in (b). Each count (N_{de}) was plotted after being normalized by an incident-photon number during 550 s in (a) or 500 s in (b). The solid curves were given by connecting the averages of five neighboring points.

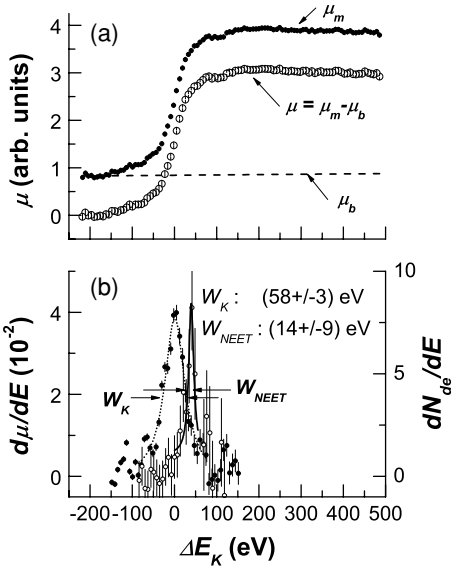

FIG. 4. Absorption coefficient (μ_m) measured in Exp. II, and the background (μ_b) are shown in (a). The open circles indicate $\mu = \mu_m - \mu_b$. A derivative, $d\mu/dE$, calculated around the gold K-edge, is plotted by the closed circle in (b). The dashed curve in (b) is its Lorentz fitting; the peak was set to the K edge ($\Delta E_K = 0$ eV). The derivative of the NEET edge observed in Exp. II, dN_{de}/dE, is also plotted in (b) by the open circle; the solid curve is its Lorentz fitting. The arrows indicate the FWHM of the NEET edge, W_{NEET}, and that of the K edge, W_K.

+474 eV and 7 eV, in Exp. II. The energy discrepancy, depending on the angle reproducibility in the monochromator, was $< \pm 6$ eV in Exp. I and $< \pm 7$ eV in Exp. II at the K edge among the scans. The data detected only with the ch-A are shown in (b) to compare the data obtained in Exp. I. The solid curves were given by connecting the averages of five neighboring points. In Fig. 4(a), the x-ray absorption spectrum of $\mu_m = \ln(I_0/I)/x$ is shown for the same energy range and steps, measured in Exp. II, where x is the sample thickness. A background μ_b of $C_1E^{-3} + C_2E^{-4}$ was estimated from μ_m between $\Delta E_K = -220$ eV and -180 eV in Fig. 4(a), where the equation was taken from an empirical relation given by Victoreen [9]; C_1 and C_2 are constants. A derivative, $d\mu/dE$, was calculated from $\mu = \mu_m - \mu_b$ and was fitted around the K edge by a Lorentz form. The closed circles and the dashed curve in Fig. 4(b) show the result. The peak position was set to the K edge. The FWHM of the K edge, W_K, was 58 $\pm$ 3 eV.

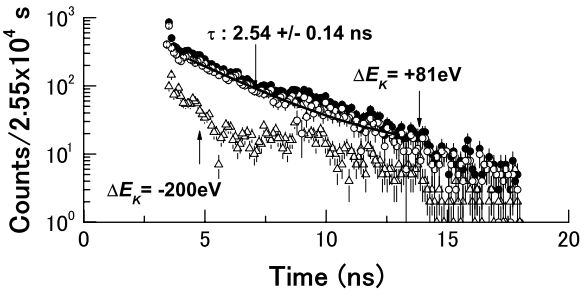

FIG. 5. Time spectrum observed in Exp. II for NEET at $\Delta E_K = +81$ eV during 25550 s (closed circles). The background (triangles) was measured at $\Delta E_K = -200$ eV. The net spectrum (open circles) was obtained by subtracting the background from the data of the closed circles, after being normalized by the incident-photon number. The solid curve shows a decay with a time-constant $\tau (= 2.54 \pm 0.14$ ns) for the data of 4.5–13 ns by a least-squares fitting.

This value corresponds to a K-shell width of (52 $\pm$ 0.7) eV [10], when considering 3.5 eV of the incident-beam width and the error. From the derivative, dN_{de}/dE, of the delayed events around the leading part in Fig. 3, the NEET edge at E_{NEET} was determined by a peak fitting of the Lorentz form. The edge was located at $\Delta E_K = +(35\pm4)$ eV for Exp. I or $+(40\pm2)$ eV for Exp. II. The FWHM of the peak was 16$\pm$14 eV or 14$\pm$9 eV, respectively. The open circles in Fig. 4(b) indicate dN_{de}/dE, obtained from the data in Exp. II; the solid curve is its fitted form. One can see that the NEET edge is located apart from the K edge and the width of the NEET edge, W_{NEET}, is quite narrow, less than one third of the K-edge width.

As the closed circles in Fig. 5, we also measured the time spectrum for NEET in order to confirm the nuclear excitation and to obtain its probability. We observed the spectrum at $\Delta E_K = +81$ eV in Exp. II, where the event rate increased sufficiently, as shown in Fig. 3(b). Another spectrum, indicated by triangles, was recorded at $\Delta E_K = -200$ eV, about four-times larger than the K-shell width, as the background for NEET. The net counts of the open circles were obtained by subtracting the data measured at $\Delta E_K = -200$ eV from that at $\Delta E_K = +81$ eV, normalized by the incident-photon number. The solid curve in Fig. 5 was given by a least-squares fitting for the same time region, as in the measurements for the resonance. The value of τ was 2.54 $\pm$ 0.14 ns, which corresponded to that observed at 77.3 keV within the errors. The experimental values obtained in Exp. II, and similarly in

TABLE I. Experimental values for the NEET probability P_{NEET}. Here, N_{ph} is the number of incident photons, N_{de} the number of the delayed events, E_{OR} the photon energy where nuclear resonance was observed, and E_{ON} the photon energy where NEET was observed. The value of E_{ON} was $\Delta E_K = +64$ eV in Exp. I or +81 eV in Exp. II, where the gold K-edge was given by $\Delta E_K = 0$ eV. Using the resonance cross section, σ_R, the value of P_{NEET} was calculated from the measured $\sigma_{\mathrm{NEET}}/\sigma_R$, the incident-beam width W, the photoelectric cross section at the K edge, σ_K, where σ_{NEET} is the NEET cross section.

	N_{ph} at E_{OR}($\times 10^{14}$)	N_{ph} at E_{ON}($\times 10^{14}$)	N_{de} at E_{OR}($\times 10^{4}$)	N_{de} at E_{ON}($\times 10^{4}$)	$\sigma_{\mathrm{NEET}}/\sigma_R$($\times 10^{-2}$)	W (eV)	P_{NEET} ($\times 10^{-8}$)
Exp. I	0.596 $\pm$ 0.011	1.377 $\pm$ 0.024	1.324 $\pm$ 0.097	0.248 $\pm$ 0.048	8.10 $\pm$ 1.68	8.8 $\pm$ 0.2	5.7 $\pm$ 1.2
Exp. II	2.869 $\pm$ 0.056	4.037 $\pm$ 0.059	[a]18.97 $\pm$ 0.39	*0.671 $\pm$ 0.089	2.51 $\pm$ 0.34	3.5 $\pm$ 0.1	4.5 $\pm$ 0.6

[a]The numbers of the events obtained only with the ch-A are shown.

Exp. I, are listed in Table I. After normalizing the delayed counts by the integral number of incident photons, the NEET probability (P_{NEET}) was given by using the same equation as Eq. (4) in Ref. [1]. The probability P_{NEET} is defined by $\sigma_{\mathrm{NEET}}/\sigma_K$, where σ_{NEET} is the NEET cross section and σ_K is the K-shell photoionization cross section [10]. We here used $f_p = (\pi \ln 2)^{1/2}$, which was adopted for the incident beam approximated by a Gaussian distribution. We also considered that the isotopic abundance of ^{197}Au was 100%. The values of P_{NEET}, $(5.7 \pm 1.2) \times 10^{-8}$ in Exp. I and $(4.5 \pm 0.6) \times 10^{-8}$ in Exp. II, agree with the previous value of $(5.0 \pm 0.6) \times 10^{-8}$ [1] within the errors.

As we have found, NEET on ^{197}Au just occurred at the energy above the K edge with a steep edge, the width of which was less than one third of the K-edge width. This is explained by the following interpretation: the NEET process occurs with a particular K-hole state, satisfying the energy condition for the nuclear resonance; also, energy conservation is strictly maintained involving the energy of an ejected photoelectron from the K shell. From the energy conservation rule between the initial and the final states, NEET occurs when the energy of the K-hole state (E_{Kh}) is the same as the sum of the nuclear transition energy (E_N) and the M_1-hole state energy (E_{M1h}). In other words, the transition to the M_1-hole state from a particular K-hole state of $E_{\mathrm{Kh}} (= E_N + E_{M1h})$ will resonantly cause the nuclear excitation. The NEET on ^{197}Au begins at the edge of E_{NEET}, which is ΔE_{NA} higher than E_K and has an energy width of W_{NEET}. Here, the energy difference between the nuclear and atomic transitions in the NEET process, ΔE_{NA}, is defined by $E_N - (E_K - E_{M1})$, where E_{M1} is the M_1-edge energy. We observed E_{NEET} of 40 eV higher than E_K in Exp. II, but ΔE_{NA} is given by 51 eV, according to the references. The absolute value of E_N may be 11 eV lower than 77.351 keV, if assuming that the absolute energies of the K and M_1 edges are correct. If ΔE_{NA} is negative in another NEET process, the NEET edge will be found at an energy of ΔE_{NA} lower than the absorption edge. The NEET transition on ^{197}Au should have an energy width depending on the widths of the initial and final states: the incident-beam width, the M_1-level width, and the level width of the excited nucleus. On the other hand, the K-shell width does not contribute to the transition. Adopting an M_1-level width of 14.3 eV (FWHM) [11], a beam width (FWHM) of 8.8 eV for Exp. I or 3.5 eV for Exp. II, and neglecting the very narrow width of the nuclear level, the observed W_{NEET} should be less than the sum of these widths, 23 or 18 eV (FWHM), according to our explanation. These values certainly exist within the experimental values, 16± 14 eV and 14±9 eV. The radiation width in the NEET transition is therefore determined by the final state width, resulting from the energy conservation requirement. This feature is analogous to resonant Raman scattering [12–14].

When the incident photon energy (E) increased over E_{NEET}, NEET continued, and fine structures of the delayed events can be seen in both Fig. 3(a) and (b). It seems that the structures corresponded to each other, although the spectrum shown in Fig. 3(a) was smeared more than that in Fig. 3(b), with a wider energy-width of the incident x-rays and with poor statistics. This feature can be explained by a common mechanism with the modulation of extended x-ray absorption fine structure (EXAFS). The EXAFS modulation means a variation of the photoabsorption rate in an ionized shell, or an interference effect produced by the outgoing photoelectron scattered from near neighboring atoms [15]. The scattering process of the photoelectron should also affect the atomic transition rate in NEET, while there is a difference in the kinetic energy of the photoelectron. At $E > E_{\mathrm{NEET}}$, the excess energy of $\varepsilon_{\mathrm{NEET}} = E - E_{\mathrm{NEET}} (= E - (E_N + E_{M1}) \geqslant 0)$ is transferred to an outgoing photoelectron emitted in NEET, according to energy conservation. The kinetic energy, ε_{ph}, of the normal photoelectron emitted from the K-shell without NEET, satisfies $E - E_K$, if neglecting the K-shell width. The energy of $\varepsilon_{\mathrm{NEET}}$ should be $\Delta E_{\mathrm{NA}} (= E_N - (E_K - E_{M1}))$ lower than ε_{ph} at the same E. A transformation of $E - \Delta E_{\mathrm{NA}}$ for the structure in NEET will give a correspondence to the EXAFS modulation at E. Moreover, since the K-shell width does not smear $\varepsilon_{\mathrm{NEET}}$, the spectrum observed in NEET will be sharper than that in the normal EXAFS. However, in the present experiments, the statistics of μ_m and of the observed NEET events were not enough for a quantitative comparison. Accurate measurements are needed to discuss in detail the relation between the NEET structure and the EXAFS modulation. Measuring the NEET events with a higher efficiency and scanning the energy of the incident x-rays stably will be more important.

We thank Prof. E. V. Tkalya for a useful discussion on the NEET mechanism. This work was performed with the approval of Japan Synchrotron Radiation Research Institute (JASRI) (Proposal No. 2001A0313-NSD-np and 2004B0783-ND3b-np) and of the Photon Factory Advisory Committee (Proposal No. 2000G022 and 2002G030). This experiment was supported in part by a Grant-in-Aid for Scientific Research from Japanese Ministry of Education, Science and Culture.

[1] S. Kishimoto *et al.*, Phys. Rev. Lett. **85**, 1831 (2000).
[2] Z. Chunmei, Nucl. Data Sheets **62**, 433 (1991).
[3] M. Morita, Prog. Theor. Phys. **49**, 1574 (1973).
[4] E. V. Tkalya, Nucl. Phys. **A539**, 209 (1992).
[5] M. R. Harston, Nucl. Phys. **A690**, 447 (2001).
[6] S. Kishimoto *et al.*, SPring-8 User Experiment Report No. 7 (2001A), p. 81.
[7] S. Kishimoto *et al.*, Nucl. Phys. **A748**, 3 (2005).
[8] J. A. Bearden, Rev. Mod. Phys. **39**, 125 (1967).
[9] J. A. Victoreen, J. Appl. Phys. **19**, 855 (1948).
[10] E. Storm and H. I. Israel, Nucl. Data Tables **A7**, 565 (1970).
[11] J. L. Campbell and T. Papp, At. Data Nucl. Data Tables **77**, 1 (2001).
[12] P. Eisenberger *et al.*, Phys. Rev. Lett. **36**, 623 (1976).
[13] T. Åberg and J. Tulkki, in *Atomic Inner-shell Physics*, edited by B. Crassmann (Plenum, New York, 1985), Chap. 10.
[14] K. Hämäläinen, D. P. Siddons, J. B. Hastings, and L. E. Berman, Phys. Rev. Lett. **67**, 2850 (1991).
[15] B. K. Teo, *EXAFS: Basic Principles and Data Analysis* (Springer-Verlag, Berlin, 1986).